

# Northumbria Research Link

Citation: Utescher, Torsten, Dreist, Andreas, Henrot, Alexandra-Jane, Hickler, Thomas, Liu, Yu-Sheng, Mosbrugger, Volker, Portmann, Felix and Salzmann, Ulrich (2017) Continental Climate Gradients in North America and Western Eurasia before and after the Closure of the Central American Seaway. *Earth and Planetary Science Letters*, 472. pp. 120-130. ISSN 0012-821X

Published by: Elsevier

URL: <http://dx.doi.org/10.1016/j.epsl.2017.05.019>  
<<http://dx.doi.org/10.1016/j.epsl.2017.05.019>>

This version was downloaded from Northumbria Research Link:  
<http://nrl.northumbria.ac.uk/30746/>

Northumbria University has developed Northumbria Research Link (NRL) to enable users to access the University's research output. Copyright © and moral rights for items on NRL are retained by the individual author(s) and/or other copyright owners. Single copies of full items can be reproduced, displayed or performed, and given to third parties in any format or medium for personal research or study, educational, or not-for-profit purposes without prior permission or charge, provided the authors, title and full bibliographic details are given, as well as a hyperlink and/or URL to the original metadata page. The content must not be changed in any way. Full items must not be sold commercially in any format or medium without formal permission of the copyright holder. The full policy is available online: <http://nrl.northumbria.ac.uk/policies.html>

This document may differ from the final, published version of the research and has been made available online in accordance with publisher policies. To read and/or cite from the published version of the research, please visit the publisher's website (a subscription may be required.)

[www.northumbria.ac.uk/nrl](http://www.northumbria.ac.uk/nrl)



## Highlights

- Neogene thermal latitudinal gradients are reconstructed for N America and W Eurasia
- Proxy-based, continental temperature gradients are evaluated against model data
- Thermal gradients were flat throughout the Miocene and strongly steepened in the Pliocene
- The thermal anomaly between North America and Europe first appeared in the Pliocene
- AMOC intensified after the final closure of the CAS during the early Pliocene

1     **Continental Climate Gradients in North America and Western Eurasia before**  
2                     **and after the Closure of the Central American Seaway**

3             Torsten Utescher<sup>1,2</sup>, Andreas Dreist<sup>2</sup>, Alexandra-Jane Henrot<sup>3</sup>, Thomas Hickler<sup>4,6</sup>, Yu-Sheng  
4             (Christopher) Liu<sup>5</sup>, Volker Mosbrugger<sup>1,4</sup>, Felix T. Portmann<sup>6</sup>, Ulrich Salzmann<sup>7</sup>

5

6     <sup>1</sup>\*Senckenberg Research Institute and Natural History Museum, Senckenberganlage 25, 60325 Frankfurt am Main, Germany

7     <sup>2</sup>Steinmann Institute, University of Bonn, Nußallee 8, 53115 Bonn, Germany

8     <sup>3</sup>Unité de Modélisation du Climat et des Cycles Biogéochimiques, University of Liège, Liège, Belgium

9     <sup>4</sup>Senckenberg Biodiversity and Climate Research Centre (SBiK-F), Senckenberganlage 25, 60325 Frankfurt am Main,  
10     Germany

11     <sup>5</sup>Research and Sponsored Projects, California State University, 1121 North State College Blvd., Fullerton, California 92831,  
12     USA

13     <sup>6</sup>Institute of Physical Geography, Goethe University Frankfurt, Altenhöferallee 1, 60438 Frankfurt am Main, Germany

14     <sup>7</sup>Department of Geography, Northumbria University, Newcastle upon Tyne, NE1 8ST, United Kingdom

15

16     \*Corresponding author:

17     Torsten Utescher, [utescher@geo.uni-bonn.de](mailto:utescher@geo.uni-bonn.de)

18

19 Abstract

20 The Gulf Stream, as part of the Atlantic Meridional Overturning Circulation (AMOC), is known as a  
21 major driver of latitudinal energy transport in the North Atlantic presently causing mild winters over  
22 northwestern Eurasia. The intensity of the AMOC throughout the Neogene, prior to the final closure  
23 of the Central American Seaway (CAS) in the early Pliocene, is still poorly known, but most authors  
24 assume that the circulation was considerably weaker than present. Here we address this issue from a  
25 continental point of view. We studied the past AMOC intensity by analyzing Neogene continental  
26 climate patterns along North American and Western Eurasian transects. Based on a total of 317  
27 palaeofloras thermal latitudinal gradients are reconstructed for three Neogene time slices, namely  
28 the middle Miocene, late Miocene, and late Pliocene using the Coexistence Approach to obtain  
29 quantitative climate data. The obtained proxy-based, continental temperature gradients are  
30 evaluated against data from a selection of published General Circulation Model (GCM) simulations  
31 for the three time slices studied.

32 Our study suggests that shallow thermal latitudinal gradients existed in North America and Western  
33 Eurasia throughout the Miocene but became strongly steepened in the late Pliocene. In both  
34 Miocene time slices studied, the higher latitudes were by up to 30 °C warmer than present (cold  
35 month mean), also at times with presumed pre-industrial CO<sub>2</sub> such as the late Miocene. In the late  
36 Pliocene high-latitude, the temperature difference with respect to the present had decreased by up  
37 to 10 °C (cold month mean). Both mean annual temperatures and cold month means of the lower  
38 mid and low latitudes were at the present-day level throughout all three time slices, or even slightly  
39 below. In both Miocene time slices, zonal temperature means at both continental transects were  
40 similar in the mid and higher latitudes. However, several northwest European sites reveal very mild  
41 winter condition suggesting the early existence of a probably less intense Palaeo-Gulf Stream. The  
42 distinct thermal anomaly (annual and cold month means) today existing between North America and  
43 Western Eurasia appeared for the first time in the late Pliocene, attaining about 50 % of the present-  
44 day magnitude. This supports the assumption that the AMOC intensified after the final closure of the

45 CAS during the early Pliocene. The results obtained from the palaeobotanical proxies are in line with  
46 data from coeval marine archives, particularly with North Atlantic sea surface temperatures (SSTs)  
47 inferred from oxygen isotopes. However, the proxy-based thermal gradients are not well reproduced  
48 by a selection of GCM simulations, due to a well-known systematic underestimation of high latitude  
49 warming by GCMs for the Miocene and Pliocene time slices.

50 Key words: Climate gradients, Northern Hemisphere, Neogene, North Atlantic Circulation, Gulf  
51 Stream, palaeobotanical record, Coexistence Approach

52

53 **1. Introduction**

54 The Gulf Stream, as part of the Atlantic Meridional Overturning Circulation (AMOC), is known as a  
55 “Heat Conveyor” and a major driver of latitudinal energy transport. The ocean current results from a  
56 combination of two systems - the wind-driven circulation and thermohaline circulation (THC) (e.g.,  
57 Manabe and Stouffer, 1995). Although the relevance of atmospheric versus oceanic heat transport to  
58 northwestern Eurasia is controversial (e.g., Seager et al., 2002) it is clear that the Gulf Stream allows  
59 “the maritime effect to operate in the northern North Atlantic and creates a milder European climate  
60 than in North America and that without the heat transport, ice would likely extend over much  
61 greater areas of ocean and land” (Rhines and Hakinnen, 2003). This effect is most pronounced in  
62 winter. Reduced salinity of surface waters related to higher precipitation rates and melting of the  
63 Greenland ice might disrupt this circulation (e.g., Johannessen et al., 2005). A slowing-down or  
64 cessation of the THC in the Northern Atlantic under future global warming may be possible and its  
65 consequences for Western Europe would be significant (e.g., Bryden et al., 2005; Rhein et al., 2013).

66 The Neogene AMOC and its varying intensity - prior to the closing of the Central American Seaway  
67 (CAS) in the early Pliocene - is still a matter of debate. Most authors state that both the circulation  
68 and associated heat transport were considerably reduced when compared to present-day conditions,  
69 the decrease of volumetric rate of transport of AMOC with an open CAS being estimated between 2  
70 to 16 Sv (e.g., Maier-Reimer et al., 1990; Lunt et al., 2007; Steppuhn et al., 2007; Sepulchre et al.,  
71 2014). However, tectonism in the Caribbean realm (Kirby et al., 2008) might have intermittently  
72 affected deep-water exchange across the CAS since middle Miocene times (Sepulchre et al., 2014;  
73 Montes et al, 2015). Considerable increases in North Atlantic Sea Surface Temperatures (SSTs) over  
74 those of the present (Lutz et al., 2008) and primary production peaks within the Northern  
75 Component Water (Poore et al., 2006; Newkirk and Martin, 2009) are already documented for the  
76 late middle to late Miocene.

77 After the closure of the CAS, both the AMOC and associated heat transport to the North Atlantic  
78 increased during the early Pliocene, due to enhanced transport of saline surface waters via an  
79 intensified Gulf Stream, and intensification of the upper North Atlantic Deep Water (NADW)  
80 formation in the Labrador Sea (Steph et al., 2006). The relative flux of deep water forming in the  
81 North Atlantic was enhanced between 4.3 and 3.7 Ma, and was warmer and more saline than today  
82 (Billups et al., 1999). The warm conditions in the late Pliocene were referred to as a stronger  
83 greenhouse and stronger conveyor (Raymo et al., 1996). The appearance of large-scale, Arctic  
84 glaciation in the Pleistocene caused a southward displacement of NADW formation or even collapse  
85 at times of fresh water pulses (Clark et al., 1999). The final establishment of the Panama land-bridge  
86 is also reflected in a decoupling of the Pacific and Atlantic  $\delta^{13}\text{C}$  records, which diverge from ca. 4.4  
87 Ma onwards (Steph et al., 2006). The Northern Atlantic circulation has and had a strong impact on  
88 the continental climate of Western Eurasia, also in times prior to the closure of the CAS (e.g., NAO-  
89 induces patterns in Tortonian records of Greece (Brachert et al., 2006), however, this impact is  
90 difficult to assess from marine proxies only.

91 In the last decade, quantitative studies of continental climate data have considerably increased in  
92 both quality and quantity. Most studies focus on the analysis of time series and therefore document  
93 climate evolution on a regional scale. Comparatively few studies exist on global or continental scale  
94 spatial palaeoclimate patterns, mainly focusing on the Paleogene (e.g., Greenwood and Wing, 1995;  
95 Fricke and Wing, 2004). For the Neogene, few studies have been carried out at a global scale. Pound  
96 et al. (2012) reconstructed the relative steepness of thermal latitudinal gradients inferred from  
97 latitudinal biome distribution in two east coast transects (the Americas / Pacific coast of Eurasia and  
98 Australia) for four time slices (Langhian, Serravallian, Tortonian, Messinian). For the late Pliocene  
99 Salzmann et al. (2008; 2013) provided global biome and climate reconstructions (mainly mean annual  
100 temperatures) for data model comparison as part of PRISM (Pliocene Research, Interpretation and  
101 Synoptic Mapping) and the Pliocene Model Inter-comparison Project (PlioMIP) (Haywood et al., 2016;  
102 Dowsett et al., 2016). However, both the Miocene and late Pliocene global vegetation

103 reconstructions use the published authors' original climate interpretations and therefore lack an  
104 internally consistent approach to derive global quantitative climate estimates from palaeobotanical  
105 proxies.

106 The study of Neogene climate patterns of Western Eurasia is the focus of the NECLIME research  
107 consortium (Bruch et al., 2007; Utescher et al., 2011). Data reconstructed for the Miocene point to  
108 shallow gradients in general, of e.g. 0.48 °C per degree latitude in the middle Miocene Western  
109 Europe, between 36 and 47 °N (Fauquette et al., 2007; Jimenez-Moreno et al., 2010), and  
110 considerably higher than present temperatures at higher mid- and higher latitudes (e.g., Bruch et al.,  
111 2011; Utescher et al., 2011). These studies represent an important knowledge base but they do not  
112 cover the required spatial range and time-frame.

113 In the present study, continental temperatures and thermal latitudinal gradients for North American  
114 and Western Eurasian transects (Fig. 1) are reconstructed from the palaeobotanical record, for a  
115 total of three Neogene time slices, namely middle Miocene, late Miocene, and late Pliocene,  
116 revealing details on Neogene cooling of the Northern Hemisphere and highlighting the apparent  
117 evolution of the effect of North Atlantic ocean circulation on Western Eurasia. Proxy-based  
118 temperature gradients are evaluated against temperature gradients obtained from a selection of  
119 published General Circulation Model (GCM) simulations. Generally, GCM simulations for Cenozoic  
120 time slices fail to reproduce the equator-to-pole temperature gradients inferred from terrestrial and  
121 marine proxy-data (Herold et al., 2010; Stephanek and Lohmann, 2012; Goldner et al., 2014) and  
122 therefore might underestimate future warming (Spicer et al., 2014). The comparison performed here  
123 allows for a first attempt to quantify the data-model mismatches for the two continental transects in  
124 the Miocene and Pliocene-

125

## 126 **2. Materials and methods**



127 To compare continental patterns on both sides of the Atlantic two transects are defined within the  
128 Northern Hemisphere. The North American transect ranges from 120 ° to 25 °W, the Western  
129 Eurasian transect from 25 °W to 35 °E. For both transects, published floral lists for a total of 317 sites  
130 were analyzed with respect to palaeoclimate. The sites were compiled to study conditions in three  
131 time intervals, the middle Miocene (15.97 – 11.63 Ma), late Miocene (11.63 – 5.33 Ma), and late  
132 Pliocene (3.6 – 2.58 Ma), and comprise micro- (pollen and spores) and macrofloras (leaves, fruits and  
133 seeds). The sites selected for both Miocene time slices in each case represent extended NECLIME  
134 data sets (records partly published in Pangaea, [www.pangaea.de](http://www.pangaea.de)), complemented by North and  
135 Central American localities (this study). Our late Pliocene time slice includes sites compiled by  
136 Salzmann et al. (2013) from palaeobotanical literature. The palaeofloras considered here have  
137 varying quality and age control. These uncertainties are accepted here in favour of spatio-temporal  
138 data cover. While the Miocene climate can be characterized as comparatively stable, a higher  
139 variability can be assumed for the late Pliocene, already having distinct glacial-interglacial cycles (e.g.,  
140 Mosbrugger et al., 2005; Zachos et al., 2008; Utescher et al., 2012; Jimenez-Moreno et al., 2013;  
141 Prescott et al., 2014; Panitz et al., 2016; Andreev et al., 2014). Details on the sites included in this  
142 study are given in the electronic supplement.

143 To reconstruct quantitative temperature data from the palaeobotanical record we use the  
144 Coexistence Approach (CA) (cf. Utescher et al., 2014 for more details on the method), together with a  
145 calibration procedure enhancing the climatic resolution (Utescher et al., 2009). Climate data for  
146 extant taxa were retrieved from the Palaeoflora Database (Utescher and Mosbrugger, 2015). As a  
147 taxonomy-dependant approach, the CA is based on climatic requirements of Nearest Living Relatives  
148 (NLRs) identified for the plant fossils. In the CA an interval is identified for a given climate variable  
149 and NLR association in a fossil flora in which a maximum number of taxa could coexist. This interval is  
150 denoted as coexistence interval representing the most probable estimation for the past climatic  
151 condition. The CA can be applied on all types of fossil floras as long as at least 10 NLRs having climate  
152 data are known. The CA is a well-established method for reconstructing Cenozoic continental spatial

153 climate patterns and time series (e.g., Mosbrugger et al., 2005; Bruch et al., 2007; 2011; Utescher et  
154 al., 2011; Popova et al., 2012; Utescher et al., 2015). The temperature resolution of the CA may  
155 attain the range of a few degrees, but depends on a variety of factors (Utescher et al., 2014).

156 Here we focus on the reconstruction of two temperature variables, cold month mean temperature  
157 (CMT) considered most sensitive to the impact of the AMOC on continental climate (e.g., Palter,  
158 2015), and mean annual temperature (MAT), a variable commonly used in model - proxy data  
159 comparisons. For the calibration procedure, we also reconstructed warm month mean temperature  
160 (WMT), in addition to MAT and CMT, as well as four precipitation variables (mean annual  
161 precipitation, MAP; precipitation of the wettest, driest and warmest month, MPwet, MPdry,  
162 MPwarm) in order to identify equivalents in modern global climate space using the 0.5° gridded  
163 climate means of New et al. (2002). The climatic sub-spaces identified for the variable combination of  
164 each palaeoflora were then used to extract calibrated MAT and CMT coexistence intervals,  
165 commonly more restricted compared to the primary CA data (Utescher et al., 2009) and therefore  
166 used in this study.

167 On average, 28 taxa ( $SD = 15$ ) contribute with climate data in the analysis, for MAT a mean resolution  
168 of 2.7 °C ( $SD = 2.4$  °C) is obtained corresponding with the average width of the coexistence intervals.  
169 For CMT the mean resolution amounts to 4.4 °C ( $SD = 4.0$  °C). This comparatively low resolution is  
170 due to the high proportion of microfloras in the record (Utescher et al., 2014). All floras included in  
171 this study are provided in the electronic supplement, including references, diversity, and climatic  
172 results encompassing both primary and calibrated data for MAT and CMT.

173 The proxy-based temperature gradients for the three periods of interest were compared to near  
174 surface air temperature gradients derived from published climate model simulations with different  
175 versions of the atmospheric model ECHAM5 (Roeckner et al., 2003). We selected available  
176 simulations of ECHAM5 with prescribed oceanic conditions or fully-coupled ocean model. The model  
177 setup follows the PLIOMIP protocol for the Pliocene simulations (Haywood et al., 2013). For Miocene

178 time slices, we selected simulations with middle-range boundary conditions, excluding e. g. extreme  
179 values of CO<sub>2</sub> concentrations or singular palaeogeography. The model simulation selection applied  
180 here allows for a first estimation of data-model mismatches for the two continental transects. Future  
181 analysis should be based on extended data-model comparison including several GCMs with various  
182 boundary conditions. We use the MPI-ESM (Krapp and Junglaus, 2011) and the Planet Simulator  
183 (Henrot et al., 2010) simulations for the middle Miocene. MPI-ESM is a comprehensive Earth-System  
184 Model including the spectral atmospheric model ECHAM5 (Roeckner et al., 2003), used here at a  
185 resolution of T42 (i.e., a resolution of 2.81°×2.81° in longitude-latitude), the land surface model  
186 (Raddatz et al., 2007; Brovkin et al., 2009), and the ocean model MPI-OM (Marsland et al., 2003).  
187 Planet Simulator is a spectral Atmospheric General Circulation Model (AGCM) derived from ECHAM5,  
188 based upon the Portable University Model of the Atmosphere, PUMA (Fraedrich et al., 1998), with a  
189 T42 resolution, and including a slab ocean model. The middle Miocene simulations assume an  
190 atmospheric CO<sub>2</sub> concentration of respectively 480 ppmv for MPI-ESM and 500 ppmv for Planet  
191 Simulator. For the late Miocene, temperature gradients are calculated from a simulation performed  
192 with the COSMOS atmosphere-ocean general circulation model (AOGCM) (Micheels et al., 2011),  
193 forced with an atmospheric CO<sub>2</sub> concentration of 360 ppmv. The atmospheric component of the  
194 model is ECHAM5 at a resolution of T31 (i.e., a resolution of 3.75°×3.75° in longitude-latitude) and  
195 the oceanic component is MPI-OM. For the late Pliocene we use two COSMOS simulations (Stepanek  
196 and Lohmann, 2012) performed in the frame of the PlioMIP project (Haywood et al., 2013). For the  
197 first simulation COSMOS 1, ECHAM5 is run in standalone mode and forced by climatological monthly  
198 means of SSTs and sea ice concentration. For the second simulation COSMOS 2, ECHAM5 is coupled  
199 to the MPI-OM ocean model. Both COSMOS late Pliocene simulations assume a CO<sub>2</sub> concentration of  
200 400 ppmv and have a T31 resolution. A summary of model setups and configurations for Miocene  
201 and Pliocene simulations is given in Table 1. More detail on the models and the designs of the  
202 climate simulations can be found in the reference publications mentioned above (Krapp and  
203 Junglaus, 2011; Henrot et al., 2010; Micheels et al., 2011; Stepanek and Lohmann, 2012).

204 To display thermal latitudinal gradients for both continental transects we calculated zonal means for  
205 MAT and CMT in steps of 5 ° latitude. For modern values we use 0.5° gridded climatological data  
206 (New et al., 2002). The model zonal and continental mean MATs and CMTs were calculated at the  
207 respective model resolutions. Only continental grid-cells (grid-cells with a land fraction greater than  
208 50 %) of the model land masks included in both transects were used to calculate the model zonal  
209 means. The visualization of the fossil gradients is also based on zonal means calculated from the  
210 means of coexistence intervals obtained from the floras in both continental transects. The mode of  
211 comparison of past and present temperature fields does not account for past elevation changes in  
212 the continental transects studied.

213

### 214 **3. Results**

#### 215 3.1 Latitudinal temperature gradients – palaeobotanical proxies

216 The spatial distribution of the fossil sites within the studied continental transects (Fig. 1) is  
217 fragmentary. While continental areas between 35 and 55 °N are well represented by data, records  
218 from the low and high latitudes are scarce, thus hampering clear identification of gradients and their  
219 inter-comparison. Today, MAT ranges from 24 to 28 °C in the low latitudes (ca. 0 – 20 °N) of both key  
220 regions (New et al., 2002). In North America, zonal MAT means in the transect decline by about 46 °C  
221 to -20 °C, at 80 °N, but in Western Eurasia by only about 33 °C, thus leading to a marked difference  
222 between both thermal gradients. This divergence is even more distinct in CMT, with North American  
223 values declining by ca. 55 °C to -32 °C at 80 °N, but in Western Eurasia by ca. 43 °C to only -18 °C at  
224 the same latitude (Fig. 1).

225 For reconstructing past climates in the low latitudes between 0 and 25 °N data from 10 palaeofloras  
226 are available. Almost all inferred temperatures are at the present-day level or even slightly lower  
227 (Chilga, Ethiopia at 12.6 °N, late Miocene; ODP Site 658, off West Africa at 21 °N, late Pliocene: by ca.  
228 2 °C for MAT) (Fig. 2). A higher value compared to the modern zonal mean is obtained only for one

229 site (Herrería flora at 17 °N, late Pliocene: by ca. 2 °C for CMT). When considering the fact that in CA  
230 reconstructions of low latitude floras the actual values are expected to be close to the warm end of  
231 the coexistence intervals we assume for the tropics a temperature level close to modern across all  
232 time slices. In both transects, the latitudinal sector from ca. 25 ° to 33 °N represents a gap in our  
233 records, except for the late Pliocene Peace Creek microflora located at ca. 28 °N on the American  
234 East Coast, providing MAT and CMT values within the range of modern conditions (Fig. 2). Overall,  
235 the mid-latitudes of our continental transects show the best data coverage although comparatively  
236 few sites are available for the eastern part of the American continent (cf. Chapter 2). For the middle  
237 Miocene high latitude sites reach 66 °N in Western Eurasia (floras on Iceland), and 72 °N in North  
238 America (Mary Sachs Gravel). Late Miocene high-latitude sites include Iceland for Western Eurasia,  
239 while data for North America are only available south of 45 °N. The late Pliocene time slice allows a  
240 comparison of both continental transects up to ca. 70 °N. Regarding the High Arctic, climate  
241 conditions can only be documented for North America (Meighen, Ellesmere Islands).

242 In both Miocene time slices, latitudinal thermal gradients were considerably shallower compared to  
243 present. Based on zonal means calculated for the palaeoclimate data by using means of coexistence  
244 intervals, a latitudinal MAT gradient of 0.23 °C/°lat ( $R^2=0.95$ ;  $SE=3.8$ ) is obtained for Western Eurasia,  
245 based on middle and late Miocene floras (modern: 0.56), for North America 0.27 °C/°lat ( $R^2=0.92$ ;  
246  $SE=5.4$ ) are obtained (modern: 0.69). For the middle and late Miocene a CMT gradient of 0.36 °C/ °N  
247 ( $R^2=0.93$ ;  $SE=3.6$ ) results for Western Eurasia, for North America 0.46 °C/°lat ( $R^2=0.91$ ;  $SE=5.6$ ;  
248 modern: 0.67; 0.92). In the lower mid-latitudes the inferred Miocene temperature plots within the  
249 range of the modern values, while almost all floras north of 40 °N indicate warmer than present  
250 conditions, with temperature anomalies (with respect to present) increasing with the latitude of the  
251 flora. The highest Miocene temperature, compared to the present zonal mean, can be found at the  
252 middle Miocene Mary Sachs Gravel megaf flora located at ca. 72 °N (ca. 25 °C for MAT, ca. 30 °C for  
253 CMT), while the Western Eurasian floras on Iceland, at ca. 66 °N, indicate MAT and CMT means  
254 warmer by ca. 10 °C than today. The zonal means calculated from our Miocene floras do not show

255 the same temperature divergence between both continental regions as we see today. For both  
256 Miocene time slices the inferred temperatures and zonal means are very similar, with the late  
257 Miocene data being slightly cooler on average. At 50 – 55 °N our reconstruction reveals differences in  
258 middle and late Miocene CMTs. The middle Miocene data includes floras with exceptionally warm  
259 CMT coexistence intervals in the order of 10-12 °C. All these refer to floras from coastal settings  
260 adjacent to the Cenozoic North Sea (Lower Rhine Basin, Lusatian Basin, Eastern North Sea Basin). In  
261 the late Miocene, such warm environmental conditions were less common by far.

262 The latitudinal thermal gradients obtained for the late Pliocene are steeper when compared to both  
263 Miocene time slices (Fig. 3). Western Eurasia shows a Pliocene MAT gradient of 0.33 °C/°lat ( $R^2=0.99$ ;  
264  $SE=1.8$ ) (CMT: 0.40;  $R^2=0.97$ ;  $SE=2.5$ ), North America has the same gradient for MAT ( $R^2=0.97$ ;  
265  $SE=4.6$ ), but a steeper CMT gradient (0.56/°lat ( $R^2=0.98$ ;  $SE=3.9$ )). The lower latitudes up to 40 °N of  
266 both transects indicate palaeotemperatures close to modern. For three sites located between 0 and  
267 25 °N temperatures were cooler than present in the order of 2 °C (eastern transect: ODP site 658  
268 (MAT); western transect: Facatativá 13 Site, Columbia, Bogotá; Bogotá B (MAT, CMT)). For Herrería  
269 (Guatemala) a warmer than present CMT (by ca. 2 °C) is reconstructed. Most of the  
270 palaeotemperatures obtained for mid-latitudinal sites north of 40 °N are clearly above the modern  
271 zonal means. However, with differences from present ranging from 2 to 5 °C, Pliocene temperatures  
272 were significantly cooler when compared to both Miocene time slices. At the high latitudes of North  
273 America both late Pliocene sites (Meighen Island, Ellesmere Island) indicate warmer than present  
274 MAT and CMT by ca. 14 °C and 20 °C, respectively. However, the temperatures are well below the  
275 Miocene estimates suggesting that late Pliocene polar temperature amplification was not as extreme  
276 as during the middle Miocene.

277 Another feature of the late Pliocene thermal gradient pattern is the appearance of the present day  
278 characteristic divergence of the gradients across both continental areas. The difference can be seen  
279 in both temperature variables studied but is more evident in CMT, attaining at least 4 °C when  
280 regarding the extremes of coexistence intervals. Although our result is based on relatively few sites

281 we assume that in the late Pliocene, the thermal difference between both continental areas attained  
282 about 50% of the present values.

283

### 284 3.2 Latitudinal temperature gradients – model data

285 Climate model simulations for the Miocene time slices show much steeper MAT and CMT gradients  
286 in both transects in comparison to data-based reconstructions. Middle and late Miocene simulations  
287 support warmer temperatures at low latitudes, and colder temperatures northwards to 50 °N, by  
288 more than 20 °C for both MAT and CMT, in comparison to the data. Between 30° and 50 °N means of  
289 model and data-based MAT and CMT fairly well agree. We calculate middle and late Miocene MAT  
290 latitudinal gradients for Western Eurasia of respectively 0.51, 0.52 and 0.54 °C/°lat for the MPI-ESM,  
291 Planet Simulator and COSMOS simulations (North America 0.59, 0.6 and 0.6). For CMT, the latitudinal  
292 gradients in Western Eurasia are respectively 0.57, 0.66 and 0.61 (North America 0.81, 0.89 and  
293 0.77). The gradients calculated from the Miocene simulations are closer to the modern ones than to  
294 the latitudinal gradients derived from the palaeobotanical data. Moreover, the modelled  
295 temperature gradients for Western Eurasia, particularly for CMT, are flatter than for North America  
296 in the middle and late Miocene simulations, suggesting a divergence of both continental regions in  
297 the Miocene simulations.

298 The temperature gradients derived from the COSMOS Pliocene simulations show a better agreement  
299 with proxy-based temperature reconstructions at mid- and high latitudes than the Miocene  
300 simulations. The latitudinal gradients calculated for Western Eurasia for MAT are respectively 0.41  
301 and 0.49°C/°lat for the COSMOS 1 and COSMOS 2 simulations (North America 0.53 and 0.59), and for  
302 CMT 0.44 and 0.51°C/°lat (North America 0.67 and 0.75). The latitudinal gradients are flatter for both  
303 continental regions in the Pliocene than in the Miocene simulations. However, as observed in the  
304 data-based temperature reconstructions, the divergence of the temperature gradients of North

305 America and Western Eurasia is more pronounced than in the Miocene runs, particularly for CMT  
306 (Fig. 3).

307

#### 308 **4. Discussion**

##### 309 4.1 Temperature gradients and patterns based on palaeobotanical proxies

310 Our reconstruction based on a total of 317 palaeobotanical records from continental areas on both  
311 sides of the Atlantic provides for the first time a coherent picture of the temperature patterns and  
312 their evolution using three selected Neogene time slices. Our data indicate that the latitudinal  
313 thermal gradients were considerably flatter than present throughout the Miocene, and steeper in the  
314 Pliocene, thus getting closer to present-day conditions. Our data also suggest the evolution of the  
315 temperature offset between North America and Western Eurasia. Partially, this offset can be related  
316 to a strengthening of the Gulf Stream causing a relative winter warming in the Eurasian continental  
317 part, combined with temperature decline in the continental interior of North America causing a  
318 relative cooling.

319 The very flat latitudinal MAT gradient we reconstruct for both Miocene time slices (ca. 0.23 °C/°lat  
320 for Western Eurasia and 0.27 °C for North America) results from the combination of near present-day  
321 low latitude temperatures and a considerable thermal anomaly at the high latitudes. The shallow  
322 inclination of both Miocene gradients resembles conditions reported for the Palaeogene (e.g.,  
323 Greenwood and Wing, 1995; Fricke and Wing, 2004) and traditionally has been related to a high  
324 atmospheric CO<sub>2</sub> level (e.g., Shellito et al., 2009). This is especially noteworthy when considering the  
325 fact that during the middle Miocene the CO<sub>2</sub> level was only moderately raised (Foster et al., 2012)  
326 while for the late Miocene most authors assume a pre-industrial level (e.g., Pagani et al., 1999; Forrest  
327 et al., 2015). Recent studies suggest therefore other mechanisms for temperature increase such as a  
328 reduction in the planetary albedo and a positive water vapor feedback in a warmer atmosphere  
329 (Knorr et al., 2011).



330 The existence of shallow latitudinal thermal gradients over most of the Miocene, combined with  
331 significantly raised temperature in the high latitudes basically coincides with results obtained in  
332 various previous studies. For Western Eurasia several studies by the NECLIME network suggest a  
333 weak Miocene climatic gradient (e.g., Bruch et al., 2007; Jimenez-Moreno et al., 2010; Utescher et  
334 al., 2011; Bruch et al., 2011; Popova et al., 2012). Pound et al. (2012) concluded from the  
335 distribution of major biomes in various Neogene time slices that the Northern Hemisphere  
336 bioclimatic zonal gradient continued to be shallower than modern throughout the Miocene and  
337 slowly became closer to modern by the Messinian. Also qualitative interpretations of the floral  
338 record in the higher latitudes (e.g. Iceland) come to the conclusion that at the onset of the late  
339 Miocene, warm temperate climate prevailed (mostly Cfa climate sensu Köppen-Geiger), supporting a  
340 vegetation with numerous thermophilous elements (Grimmson et al., 2007). In Iceland, warmth-  
341 loving taxa including *Magnolia*, *Liriodendron*, *Sassafras* and *Comptonia* went extinct between 12 and  
342 10 Ma, following the cooling after the Mid-Miocene Climatic Optimum (MMCO). However, this  
343 association was replaced by another set of thermophilous taxa (Juglandaceae aff.  
344 *Pterocarya/Cyclocarya*, *Rhododendron ponticum* type; cf. Denk et al., 2005) at 10 Ma. More evidence  
345 for the exceptionally warm higher latitudes comes from the middle Miocene fossil record of Jutland  
346 where palms are reported among other thermophilous floral elements (Friijs, 1975; Larsson et al.,  
347 2011). The presence of crocodiles and apes in the Langhian of the Lower Rhine Basin (Mörs et al.,  
348 2000) and a very warm climatic phase in the late Tortonian (Lower Rhine Basin, 7 F horizon  
349 containing fossil taxa referred to the *Mastixia* genus, and other thermophilous components (see van  
350 der Burgh, 1988) provide another line of evidence.

351 Temperatures similar to those of the present level in the lower latitude Miocene sites, namely  
352 localities of the Tethyan realm, were previously described in other studies using the CA to quantify  
353 palaeoclimate (e.g. Mantzouka et al., 2015). In our reconstruction, the Miocene temperature  
354 gradients form a plateau in the latitudinal range of the Tethyan realm (Fig. 2), pointing to equable  
355 conditions in this region and to temperatures close to modern. Other studies carried out on middle

356 to late Miocene floras of Western Europe located between 36 and 47 °N came to somewhat differing  
357 conclusion. Based on the Climate Amplitude Method (Fauquette et al., 1998), a MAT level in the  
358 western Mediterranean realm consistently warmer by 4 °C compared to modern values and a  
359 steeper gradient (0.48; 0.6 °C /°lat) were reconstructed (Fauquette et al., 2007; Jimenez-Moreno et  
360 al., 2010).

361 No comprehensive quantitative data on latitudinal temperature gradients currently exist for North  
362 American Miocene floras. This lack of information might result from the scarcity of coeval sites in the  
363 eastern half of the continent, a fact that also compromises the present analysis. Moreover, climatic  
364 analyses for the sites located in western North America are complicated by uncertainties concerning  
365 the palaeoaltitude of the different basin complexes (e.g., McMillan et al., 2006). Based on the  
366 occurrence of thermophilous taxa in mid-Miocene Pacific floras located between 35 and 65 °N, a  
367 latitudinal gradient of 0.3 °C per degree of latitude has been estimated by Liu and Leopold (1994), a  
368 value close to our reconstruction. Although being based on few northerly sites only, our gradient  
369 points to conditions comparable with Western Eurasia. For the low latitudes between 10 and 20 °  
370 data for both Miocene time slices indicate temperatures close to the modern ones. However, it is  
371 important to note that the NLR-based CA does not allow for reconstructing warmer conditions than  
372 the present global maximum (Utescher et al., 2014).

373 For the late Pliocene our data suggest warmer than present conditions for the higher mid- and higher  
374 latitudes. This coincides with a raised CO<sub>2</sub> level (Martínez-Botí et al., 2015; Pagani et al., 2010). For  
375 Western Europe our reconstruction partly agrees with the data provided by Fauquette et al. (2007)  
376 suggesting MATs at 45 – 50 °N ca. 2 – 3 °C higher than present while in our reconstruction, MATs for  
377 the more southerly sites (e.g., the Andalucia G1 site) were near the modern level, thus indicating a  
378 shallower thermal gradient. Accordingly, palaeobotanical data for the tropical zone suggest that the  
379 evergreen rain forest belt was nearly in the same latitudinal position as today (e.g., Kershaw and  
380 Sluiter, 1982; Suc et al., 1995). At high latitudes, the late Pliocene warm climate resulted in taiga  
381 forest, and positioned the taiga – tundra transition zone 2,500 km (Canadian Arctic) further north

382 compared to present (e.g., DeVernal and Mudie, 1989; Salzmann et al. 2008). For the Canadian high  
383 Arctic, a multi-proxy study suggests Pliocene MATs were approximately 19 °C warmer than at present  
384 (Ballantyne et al., 2010; according to our data: 20 – 23 °C). However, with zonal CMT means in the  
385 order of -10 to -18 °C, as calculated for the sites at 70 - 80 °N, our results accommodate Arctic sea ice  
386 forming during the Pliocene (e.g., Lunt et al., 2008; Meyers and Hinnov, 2010).

387

#### 388 4.2 Evolving offset between the latitudinal gradients

389 The temperature difference between both continental areas reflected in modern climatology (Fig. 1;  
390 New et al., 2002) can be related to the oceanic circulation in the North Atlantic and its intensity,  
391 being an important trigger for the observed offset of the temperature gradients. The present-day  
392 very effective Gulf Stream, with a capacity of up to 150 sv adds to the shallow modern gradient in  
393 Western Eurasia and causes winter temperatures allowing palm growth on the Kerry coast of Ireland,  
394 at a northern latitude of 53 °N. Since palaeogeography has not substantially changed in our selected  
395 transects throughout the Neogene, the evolving differences can be interpreted to reflect past  
396 changes in the Gulf Stream intensity.

397 According to our present results, there is first clear evidence for the offset of latitudinal thermal  
398 gradients between both transects in the late Pliocene (fig. 2). This points to a Pliocene intensification  
399 of the Gulf Stream postdating the final closure of the CAS between 4.3 and 3.7 Ma (Kirby et al., 2008)  
400 as is suggested based on marine proxies (increased Atlantic THC, intensified Upper NADW formation  
401 in the Labrador Sea, and decoupling of the Pacific and Atlantic  $\delta^{13}\text{C}$ ; cf. Steph et al., 2006).

402 Considering the fact that this offset is about 50 % of the present, our data do not support a stronger-  
403 than-present conveyor as proposed for the time of the late Pliocene warmth (Raymo et al., 1996;  
404 Billups et al., 1999).

405 When comparing CMT data obtained for the middle Miocene Pyramid Lake flora (CMT 5.0 – 5.1 °C)  
406 with Western European floras at the same latitude (e.g., several of the LRB and WB floras: CMT ca. 9

407 – 12 °C) the temporary existence of a Palaeo-Gulf Stream, already in the late early to middle Miocene  
408 appears possible. Similar observations were made by Bruch et al. (2011) reporting low seasonality for  
409 Western Europe during the Burdigalian and Langhian. Moreover, there is evidence for milder  
410 conditions in Western Eurasia and a more thermophilous aspect of the vegetation compared to the  
411 eastern part of North America at the same latitude (Utescher et al., 2013). Recent studies comparing  
412 mid-latitude Eurasian records of the Atlantic and Pacific sides of Eurasia came to the conclusion that  
413 a marked temperature difference (mainly CMT) between both regions began to evolve during the  
414 Aquitanian, attaining more than 5 °C for CMT during the Mid Miocene Climatic Optimum (Utescher et  
415 al., 2015). This temperature difference between East and West suggests the existence of a Palaeo-  
416 Gulf Stream, already operational from the late early Miocene on. This agrees with evidence for an  
417 earlier, at least intermittent, disappearance of the CAS, at ca. 15 Ma (Montes et al., 2015; Bacon et  
418 al., 2013).

419

#### 420 4.3 Proxy-based gradients and palaeoclimate modelling

421 As is shown by our proxy-model data comparison at the level of zonal means, middle and late  
422 Miocene simulations do not reproduce the latitudinal thermal gradients reconstructed from  
423 palaeobotanical data both in North America and Western Eurasia. The model gradients are closer to  
424 the modern ones, due to slightly warmer temperature at low latitudes and much colder  
425 temperatures at high latitudes compared to the data-based reconstructions. Previous studies already  
426 pointed out that the models underestimate proxy-derived mean annual temperatures for the middle  
427 Miocene and overestimate the equator-to-pole temperature gradient (Herold et al., 2010; Goldner et  
428 al., 2014; Henrot et al., 2016). Goldner et al. (2014) reported that most of the models simulate only  
429 one third of the expected middle Miocene warming, suggesting that GCMs are either not sensitive  
430 enough or additional feedbacks remain missing to simulate the Miocene warmth. The inability of  
431 models to reproduce Cenozoic climates in general can also be attributed to the calibration of the

432 models to present-day climate, using various forms of often simplifying parameterizations (Stainforth  
433 et al., 2005; Spicer et al., 2013). However, some model-data mismatches can also be due to feedback  
434 mechanisms in the climate system of the models. For example, the MPI-ESM and COSMOS Miocene  
435 simulations produce temperatures close to the modern ones or even slightly cooler in Northwestern  
436 Europe, in response to a weakening of the meridional heat transport in the North Atlantic resulting  
437 from a reduction of NADW production caused by sea-ice melting under higher  $p\text{CO}_2$  (Krapp and  
438 Jungclaus, 2011; Butzin et al., 2011).

439 All the selected Miocene simulations show a steeper thermal gradient in North America in  
440 comparison to Western Eurasia, reflecting the continental influence on temperature in North  
441 America (Henrot et al., 2010; Krapp and Jungclaus, 2011).

442 The late Pliocene experiments are in better agreement with the proxy data reconstructions, but e.g.  
443 for the high latitudes of North America, model estimates are still too cold by ca. 8 °C compared to the  
444 proxy-based zonal mean. In the Pliocene simulations, the difference in temperature gradients  
445 between North America and Western Eurasia is well marked. The thermal gradient is close to the  
446 Miocene ones in North America, but is much flatter in Western Eurasia, in response to the enhancing  
447 of the Gulf Stream effect with a closed CAS (Haywood et al., 2013; Stepanek and Lohmann, 2012).  
448 The gradient is steeper in the fully coupled ocean-atmosphere simulation COSMOS 2, because the  
449 oceanic model cannot reproduce the warming in the northern North Atlantic Ocean and  
450 neighbouring areas of the Arctic suggested by sea surface temperature proxy-based reconstructions  
451 (Dowsett et al., 2013), which are prescribed in the atmosphere-only COMSOS 1 simulation (Stepanek  
452 and Lohmann, 2012). This leads to a better agreement of the atmosphere-only COSMOS 1 simulation  
453 with proxy data reconstructions.

454

455 4.4 Marine proxies

456 Marine data represent important independent proxies to assess the reliability of the palaeobotany  
457 based reconstruction of thermal gradients although they are as well subject to various uncertainties  
458 (e.g., cf. Crowley and Zachos (2000) for planctonic forams). From various studies on Cenozoic  
459 continental climate evolution, a close correlation with marine archives could be demonstrated at  
460 different scales (e.g., Mosbrugger et al., 2005; Donders et al., 2009; Utescher et al., 2012). Also the  
461 shallow latitudinal gradients evidenced by continental data, including the warmer-than-present high  
462 latitudes for all the time slices, are largely supported by proxy-based sea surface temperature data  
463 (SSTs) available from boreholes in the North Atlantic.

464 For the middle Miocene between 14 and 17 Ma, including the MMCO, several studies indicate warm  
465 SSTs for the North Atlantic ranging between 15° and 22 °C at ca 50 °N (e.g., Pagani et al., 1999;  
466 Shevenell et al., 2004; Raddatz et al., 2011). These estimates are in perfect agreement with our  
467 reconstruction of continental Western European MATs of 15.9 °C (SD = 1.3 °C) as an average  
468 obtained for that latitude. At high northern latitudes there is evidence for high SST anomalies  
469 increasing with latitude (Robinson et al., 2008; Oleinik et al., 2008; Pohlmann et al., 2009), supporting  
470 our data.

471 Multi-proxy SST estimates document warm surface water conditions in the higher mid- and high  
472 latitudes of the North Atlantic during the late Pliocene (cf. Lawrence et al., 2009; DSDP sites 606, 607,  
473 609, 552). At site 552, ca. 58 °N, south of Iceland, a  $\Delta$ SST of ca. 5 – 7 °C with respect to present is  
474 reported, similar to the continental  $\Delta$ MAT of >6 °C we reconstruct for the Sleipner well. Strong,  
475 sustained cooling of North Atlantic SSTs, e.g. by ~4.5 °C at around 3.5 Ma (Site 982; Lawrence et al.,  
476 2009) postdates most of our proxy data records.

477

## 478 **5. Conclusions**

479 Our study shows that the shallow thermal gradients that existed in North America and Western  
480 Eurasia throughout the Miocene strongly steepened in the late Pliocene. In both the middle and late

481 Miocene time slice, the higher mid and high latitudes were considerably warmer than present,  
482 independent of prevailing atmospheric pCO<sub>2</sub> conditions, including pre-industrial concentrations  
483 suggested for the late Miocene, or under raised atmospheric CO<sub>2</sub> reconstructed by most of the  
484 authors for the time of the MMCO. The MAT anomaly at high northern latitudes with respect to  
485 present (at 75 – 80 °N) declined from about 30 °C in the Miocene to about 20 °C in the late Pliocene.  
486 Hence, very warm high latitudes persisted in the study area throughout most of the Neogene.

487 According to our continental data, temperatures of the lower mid and low latitudes were at the  
488 present-day level, or even a few degrees below. Thus, the thermal gradients reconstructed based on  
489 zonal means of the palaeobotany-based proxies asymptotically approximate modern continental  
490 gradients at northern latitudes between 34 to 40 °.

491 Our reconstruction is basically in line with other estimates of continental temperatures for the  
492 studied time slices based on the palaeobotanical record such as the distribution of major zonal  
493 biomes. Past scenarios with generally raised continental temperatures under higher atmospheric  
494 pCO<sub>2</sub>, including the lower latitudes, are not supported by our reconstruction. Moreover, the  
495 continental temperature patterns inferred from palaeobotanical data largely agree with results  
496 obtained from coeval marine archives, particularly with North Atlantic SSTs inferred from oxygen  
497 isotopes. However, the proxy-based thermal gradients are not well reproduced by a selection of GCM  
498 simulations for the studied time slices. Model simulations show steeper temperature gradients,  
499 particularly for the Miocene, mainly due to an underestimation of high latitude warming in  
500 comparison to data-based reconstructions.

501 According to our results there is evidence that the distinct thermal anomaly presently existing  
502 between North America and Western Eurasia evolved after the late Miocene, attaining about 50 % of  
503 the present-day magnitude in the late Pliocene. The difference between both continental regions is  
504 most expressed in winter temperature and is considered to reflect both the degree of winter cooling  
505 in the high latitude continental interior of North America as well as the effect of the Gulf Stream

506 creating mild winter conditions in northwestern Eurasia. Thus, the first appearance of the difference  
507 in the late Pliocene continental proxies supports the assumption that AMOC intensified after the final  
508 closure of the CAS during the early Pliocene. However, very warm CMTs reconstructed for several  
509 northwest European Miocene sites suggest that there existed a Miocene Palaeo-Gulf Stream  
510 circulation that caused mild winter in coastal areas of the Cenozoic North Sea.

511 Although a large number of sites was compiled to analyse past continental climate patterns our study  
512 reveals distinct gaps in the palaeobotanical record of both transects. Future works will mainly focus  
513 on the palaeobotanical record of the North American continental transect in order to enhance data  
514 cover and taxonomic resolution in the available palaeofloras.

515

## 516 **Acknowledgements**

517 We thank our colleagues from the NECLIME (Neogene Climate Evolution in Eurasia) consortium for  
518 contributing with proxy data and lively discussions. We are grateful to the School of Earth and  
519 Environment, University of Leeds (UK), the PliomIP project, and Mario Krapp for sharing modeling  
520 data. We are very thankful to Robert A. Spicer and an anonymous reviewer for valuable comments  
521 and suggestions. The financial support of the German Science Foundation (DFG) is gratefully  
522 acknowledged (project MI 926/8-1).

523

## 524 **References**

525 Andreev, A.A., Tarasov, P.E., Wennrich, V., Raschke, E., Herzschuh, U., Nowaczyk, N.R., Brigham-  
526 Grette, J., Melles, M., 2014. Late Pliocene and Early Pleistocene vegetation history of northeastern  
527 Russian Arctic inferred from the Lake El'gygytyn pollen record. *Climate of the Past* 10, 1017–1039.



528 Bacon, C., Mora, A., Wagner, W.L., Jaramillo, C., 2013. Testing a new geological model of evolution of  
529 the Isthmus of Panama in a phylogenetic framework using palms (Arecaceae). *Bot. J. Linn. Soc.* 171,  
530 287–300.

531 Billups, K., Ravelo, A.C., Zachos, J.C., Norris, R.D., 1999. Link between oceanic heat transport,  
532 thermohaline circulation, and the Intertropical Convergence Zone in the early Pliocene Atlantic.  
533 *Geology* 27, 319-322.

534 Brachert, T.C., Reuter, M., Felis, T., Kroeger, K.F., Lohmann, G., Micheels, A., 2006. Porites corals from  
535 Crete (Greece) open a window into Late Miocene (10 Ma) seasonal and interannual climate  
536 variability. *Earth and Planetary Science Letters* 245, 81–94.

537 Brovkin, V., Raddatz, T., Reick, C., Claussen, M., Gayler, V., 2009. Global biogeophysical interactions  
538 between forest and climate. *Geophys. Res. Lett.* 36, L07405.

539 Bruch, A.A., Uhl, D., Mosbrugger, V., 2007. Miocene Climate in Europe - Patterns and Evolution.  
540 *Palaeogeography, Palaeoclimatology, Palaeoecology*, 253, 1–7.

541 Bruch, A.A., Utescher, T., Mosbrugger, V., NECLIME members, 2011. Precipitation patterns in the  
542 Miocene of Central Europe and the development of continentality. *Palaeogeogr. Palaeoclimatol.*  
543 *Palaeoecol.* 304, 202–211.

544 Bryden H., Longworth H., Cunningham S., 2005. Slowing of the Atlantic meridional overturning  
545 circulation at 25° N. *Nature* 438, 655–657.

546 Butzin, M., Lohmann, G., Bickert, T., 2011. Miocene ocean circulation inferred from marine carbon  
547 cycle modeling combined with benthic isotope records. *Paleoceanography* 26, PAI203.

548 Van der Burgh, J., 1988. Some local floras from the Neogene of the Lower Rhenish Basin: *Journal of*  
549 *Tertiary Research* 9, 181–212.

550 Clark, P.U., Alley, R.B., Pollard, D., 1999. Northern Hemisphere Ice-Sheet Influences on

551 Global Climate Change. *Science* 286, 1104–1111.

552 Crowley, T.J., Zachos, J.C., 2000. Comparison of zonal temperature profiles for past warm time  
553 periods. In: Huber, B., MacLeod, K., Wing, S. (eds): *Climates of warm time periods*. Cambridge  
554 University Press, Cambridge, UK, pp. 50–76.

555 Denk, T., Grímsson, F., Kvacek, Z., 2005. The Miocene floras of Iceland and their significance for late  
556 Cainozoic North Atlantic biogeography. *Bot. J. Linn. Soc.* 149, 369–417.

557 Donders, T.H., Weijers, J.W.H., Munsterman, D.K., Kloosterboer-van Hoeve, M.L., Buckles, L., Pancost,  
558 R.D., Sinninghe Damsté, J.S., Brinkhuis, H., 2009. Strong climate coupling of terrestrial and marine  
559 environments in the Miocene of northwest Europe. *Earth and Planetary Science Letters* 281, 215–  
560 225.

561 Dowsett, H.J., Barron, J.A., Poore, R.Z., Thompson, R.S., Cronin, T.M., Ishman, S.E., Willard, D.A.,  
562 1999. Middle Pliocene Paleoenvironmental Reconstruction: PRISM2. U.S. Geological Survey Open  
563 File Report, 99–535.

564 Dowsett, H.J., Foley, K.M., Stoll, D.K., Bentsen, M., Otto-Bliesner, B.L., Bragg, F.J., Chan, W., Chandler,  
565 M.A., Contoux, C., Jonas, J.A., Jost, A., Kamae, Y., Lohmann, G., Lunt, D.J., Nisancioglu, K.H., Abe-  
566 Ouchi, A., Ramstein, G., Riesselman, C.R., Robinson, M.M., Rosenbloom, N.A., Salzmann, U., Sohl, L.,  
567 Stepanek, C., Strother, S.L., Ueda, H., Ying, Q., Zhang, Z., 2013. Sea Surface Temperature of the mid-  
568 Piacenzian Ocean: A Data-Model Comparison. *Scientific Reports* 3, doi:10.1038/srep02013.

569 Dowsett, H., Dolan, A., Rowley, D., Pound, M., Salzmann, U., Robinson, M., Chandler, M., Foley, K.,  
570 Haywood, A., (2016). The PRISM4 (mid-Piacenzian) palaeoenvironmental reconstruction, *Climate of*  
571 *the Past Discussions*. doi:10.5194/cp-2016–33.

572 Fauquette, S., Suc, J.-P., Jiminez-Moreno, G., Favre, E., Jost, A., Micheels, A., Bachiri-Taoifiq, N.,  
573 Bertini, A., Clet-Pellegrin, M., Diniz, F., Farjanel, G., Feddi, N., Zheng, Z., 2007. Latitudinal climatic  
574 gradients in Western European and Mediterranean regions from the Mid-Miocene (~15 Ma) to the

575 Mid-Pliocene (~3.6 Ma) as quantified from pollen data. In: Williams, M., Haywood, A.M., Gregory,  
576 F.J., Schmidt, D.N. (Eds.), *Deep-Time Perspectives on Climate Change: Marrying the Signal from*  
577 *Computer Models and Biological Proxies*. The Micropalaeontological Society, Special Publications.  
578 The Geological Society, London, pp. 481–502.

579 Fauquette, S., Guiot, J., Suc, J.-P., 1998. A method for climatic reconstruction of the Mediterranean  
580 Pliocene using pollen data. *Palaeogeography, Palaeoclimatology, Palaeoecology* 144, 183–201.

581 Forrest, M., Eronen, J.T., Utescher, T., Knorr, G., Stepanek, C., Lohmann, G., Hickler, T., 2015. Climate-  
582 vegetation modelling and fossil plant data suggest low atmospheric CO<sub>2</sub> in the late Miocene. *Climate*  
583 *of the Past* 11, 1701–1732.

584 Foster, G.L., Lear, C.H., Rae, J.W.B., 2012. The evolution of pCO<sub>2</sub>, ice volume and climate during the  
585 middle Miocene. *Earth and Planetary Science Letters* 341–344, 243–254.

586 Fraedrich, K., Kirk, E., Lunkeit, F., 1998. PUMA Portable University Model of the Atmosphere. Tech.  
587 Rep. 16, Meteorologisches Institut, Universität Hamburg, Hamburg.

588 Fricke, H.C., Wing, S.L., 2004. Oxygen isotope and paleobotanical estimates of temperature and  
589 δ<sup>18</sup>O-latitude gradients over North America during the early Eocene. *American Journal of Science*  
590 304, 612–635.

591 Friis, E.M., 1975. Climatic implications of microcarpological analysis of the Miocene FASTERHOLT flora,  
592 Denmark. *Bulletin of the Geological Society of Denmark* 24, 179–191.

593 Goldner, A., Herold, N., Huber, M., 2014. The challenge of simulating the warmth of the mid-Miocene  
594 climatic optimum in CESM1. *Clim. Past* 10, 523–536.

595 Greenwood, D.R., Wing, S.L., 1995. Eocene continental climates and latitudinal temperature  
596 gradients. *Geology* 23, 1044–1048.

597 Grimsson, F., Simonarson, L.A., Denk, T., 2007. Late Langhian to early Serravallian floras of Iceland.  
598 *Naturufraedingurinn* 75, 85–106.

599 Haywood, A. M., Hill, D. J., Dolan, A. M., Otto-Bliesner, B. L., F. Bragg, F., Chan, W.-L., Chandler, M.  
600 A., C. Contoux, C., H. J. Dowsett, H. J., Jost, A., Kamae, Y., Lohmann, G., Lunt, D. J., Abe-Ouchi, A.,  
601 Pickering, S. J., Ramstein, G., Rosenbloom, N. A., Salzmann, U., Sohl, L., Stepanek, C., Ueda, H., Yan,  
602 Q., Zhang, Z., 2013. Large-scale features of Pliocene climate: results from the Pliocene Model  
603 Intercomparison Project. *Clim. Past*, 9, 191–209.

604 Haywood, A. M., Dowsett, H. J., Dolan, A. M., Rowley, D., Abe-Ouchi, A., Otto-Bliesner, B., Chandler,  
605 M. A., Hunter, S. J., Lunt, D. J., Pound, M., and Salzmann, U., 2016. Pliocene Model Intercomparison  
606 (PlioMIP) Phase 2: scientific objectives and experimental design, *Climate of the Past* 12, 663–675.

607 Henrot, A.-J., François, L., Favre, E., Butzin, M., Ouberdous, M., Munhoven, G., 2010. Effects of CO<sub>2</sub>,  
608 continental distribution, topography and vegetation changes on the climate at the Middle Miocene: a  
609 model study. *Clim. Past* 6, 675–694.

610 Henrot, A.-J., Utescher, T., Erdei, B., Dury, M., Hamon, N., Ramstein, G., Krapp, M., Herold, N.,  
611 Goldner, A., Favre, E., Munhoven, G., François, L., 2016. Middle Miocene climate and vegetation  
612 models and their validation with proxy data. *Palaeogeography, Palaeoclimatology, Palaeoecology*.  
613 doi: 10.1016/j.palaeo.2016.05.026.

614 Herold, N., Müller, R., Seton, M., 2010. Comparing early to middle Miocene terrestrial climate  
615 simulations with geological data. *Geosphere* 6 (6), 952–961.

616 Jiménez-Moreno, G., Fauquette, S., Suc, J.-P., 2010. Miocene to Pliocene vegetation reconstruction  
617 and climate estimates in the Iberian Peninsula from pollen data. *Review of Palaeobotany and*  
618 *Palynology* 162, 403–415.

619 Johannessen, O.M., Khvorostovsky, K., Miles, M.W., L.P. Bobylev, 2005. Recent Ice-Sheet Growth in  
620 the Interior of Greenland. *Science* 310, 1013–1016.

621 Kirby, M.X., Jones, D.S., MacFadden, B.J., 2008. Lower Miocene stratigraphy along the Panama Canal  
622 and its bearing on the Central American Peninsula. *PLoS ONE* 3(7), e2791.

623 Krapp, M., Jungclaus, J., 2011. The Middle Miocene climate as modelled in an atmosphere-ocean-  
624 biosphere model. *Clim. Past* 7, 1169–1188.

625 Larsson, L.M., Dybkjær, K., Rasmussen, E.S., Piasecki, S., Utescher, T., Vajda, V., 2011. Miocene  
626 climate evolution of northern Europe: A palynological investigation from Denmark. *Palaeogeography,*  
627 *Palaeoclimatology, Palaeoecology* 309, 161–175.

628 Lawrence, K.T., Herbert, T.D., Brown, C.M., Raymo, M.E., Haywood, A. M., 2009. High-amplitude  
629 variations in North Atlantic sea surface temperature during the early Pliocene warm Period.  
630 *Paleoceanography* 24, PA2218, doi:10.1029/2008PA001669.

631 Lunt, D., Valdés, P., Haywood, A., Rutt, I., 2007. Closure of the Panama Sea-way during the Pliocene:  
632 implications for climate and Northern Hemisphere glaciation. *Climate Dynamics* 30, 1–18.

633 Lunt, D.J., Flecker, R., Valdes, P.J., Salzmann, U., Gladstone, R., Haywood, A.M., 2008. A methodology  
634 for targeting palaeo proxy data acquisition: A case study for the terrestrial late Miocene, *Earth and*  
635 *Planetary Science Letters* 271, 53–62.

636 Lutz, B.P., Ishman, S.E., Dowsett, H.J., 2008. Late Miocene to early Pliocene planktonic foraminiferal  
637 sea surface temperature estimates from DSDP Site 103 (northern Blake-Bahama Outer Ridge) based  
638 upon the Modern Analog Technique. American Geophysical Union, Fall Meeting 2008, abstract  
639 PP21B–1431.

640 Maier-Reimer, E., Mikolajewicz, U., Crowley, T., 1990. Ocean General Circulation Model Sensitivity  
641 Experiment with an open Central American Isthmus. *Palaeoceanography* 5, 349–366.

642 Manabe, S., Stouffer, R.J., 1995. Simulation of abrupt climate change induced by freshwater input to  
643 the North Atlantic Ocean. *Nature* 378, 165–167.

644 Mantzouka, D., Kvaček, Z., Teodoridis, V., Utescher, T., Tsapas, N., Karakitsios, V., 2015. A new late  
645 Miocene (Tortonian) flora from Gavdos Island in southernmost Greece evaluated in the context of  
646 vegetation and climate in the Eastern Mediterranean. *Neues Jahrbuch für Geologie und*  
647 *Paläontologie - Abhandlungen* 275, 47–81.

648 Marsland, S.H.H., Jungclaus, J., Latif, M., Röske, F., 2003. The Max-Planck-Institute global ocean/sea  
649 ice model with orthogonal curvilinear coordinates. *Ocean Modelling* 5, 91–127.

650 Martínez-Botí, M.A., Foster, G.L., Chalk, T.B., Rohling, E.J., Sexton, P.F., Lunt, D.J., Pancost, R.D.,  
651 Badger, M.P.S., Schmidt, D.N., 2015. Plio-Pleistocene climate sensitivity evaluated using high-  
652 resolution CO<sub>2</sub> records. *Nature* 518, 49–54. doi:10.1038/nature14145

653 McMillan, M.E., Heller, P.L., Wing, S.L., 2006. History and causes of post-Laramide relief in the Rocky  
654 Mountain orogenic plateau. *Geol. Soc. Am. Bull.* 118, 393–405.

655 Meyers, S.R., Hinnov, L., 2010. Northern Hemisphere glaciation and the evolution of Plio-Pleistocene  
656 climate noise. *Paleoceanography* 25, PA3207.

657 Micheels, A., Bruch, A., Eronen, J., Fortelius, M., Harzhauser, M., Utescher, T., Mosbrugger, V., 2011.  
658 Analysis of heat transport mechanisms from a Late Miocene model experiment with a fully-coupled  
659 atmosphere–ocean general circulation model. *Palaeogeogr., Palaeoclimatol., Palaeoecol.* 304, 337–  
660 350.

661 Mörs, T., von der Hocht, F., Wutzler, B., 2000. Die erste Wirbeltierfauna aus der miozänen  
662 Braunkohle der Niederrheinischen Bucht (Vilse-Schichten, Tagebau Hambach). *Paläontologische*  
663 *Zeitschrift* 74, 145–170.

664 Montes, C., Cardona, A., Jaramillo, C., Pardo, A., Silva, J.C., Valencia, V., Ayala, C., Pérez-Angel, L.C.,  
665 Rodríguez-Parra, L.A., Ramirez, V., Niño, H., 2015. Middle Miocene closure of the Central American  
666 Seaway. *Science* 348, 226–229.

667 Mosbrugger, V., Utescher, T., Dilcher, D.L., 2005. Cenozoic continental climatic evolution of Central  
668 Europe. *Proceedings of the National Academy of Sciences* 102, 14964–14969.

669 New, M., Lister, D., Hulme, M., Makin, I., 2002. A high-resolution data set of surface climate over  
670 global land areas. *Climate Research* 21, 1–25.

671 Newkirk, D.R., Martin, E.E., 2009. Circulation through the Central American Seaway during the  
672 Miocene carbonate crash. *Geology* 37, 87–90.

673 Oleinik, A., Marincovich, L., Barinov, K.B., Swart, P.K., 2008. Magnitude of Middle Miocene warming  
674 in North Pacific high latitudes: stable isotope evidence from *Kaneharaia* (*Bivalvia*, *Dosiniinae*).  
675 *Bulletin of the Geological Survey of Japan* 59, 339–353.

676 Pagani, M., Liu, Z., LaRiviere, J., Ravelo, A.C., 2010. High Earth-system climate sensitivity determined  
677 from Pliocene carbon dioxide concentrations. *Nat. Geosci.* 3, 27–30.

678 Pagani, M., Freeman, K.H., Arthur, M.A., 1999. Late Miocene Atmospheric CO<sub>2</sub> Concentrations and  
679 the Expansion of C<sub>4</sub> Grasses. *Science* 285, 876–879.

680 Palter, J.B., 2015. The Role of the Gulf Stream in European Climate. *Annual Review of Marine Science*  
681 7, 113–37.

682 Panitz, S., Salzmann, U., Risebrobakken, B., De Schepper, S., Pound, M.J., 2016. Climate variability  
683 and long-term expansion of peatlands in Arctic Norway during the late Pliocene (ODP Site 642,  
684 Norwegian Sea). *Climate of the Past* 12, 1043–1060.

685 Pohlman, E.E., Lawrence, K., Herbert, T., 2009. Temperature and productivity records from the late  
686 Miocene North Atlantic. *Geological Society of America Abstracts with Programs* 41 (3), p. 35.

687 Poore, H.R., Samworth, R., White, N.J., Jones, S.M., McCave, I.N., 2006. Neogene overflow of  
688 Northern Component Water at the Greenland-Scotland Ridge. *Geochemistry, Geophysics*  
689 *Geosystems* 7,Q06010, doi:10.1029/2005 GC00 1085

690 Popova, S., Utescher, T., Gromyko, D., Bruch, A.A., Mosbrugger, V., 2012. Palaeo-climate evolution in  
691 Siberia and the Russian Far East from the Oligocene to Pliocene – evidence from fruit and seed floras.  
692 *Turk. J. Earth Sci.* 21, 315–334.

693 Pound, M.J., Haywood, A.M., Salzmann, U., Riding, J.B., 2012. Global vegetation dynamics and  
694 latitudinal temperature gradients during the mid to Late Miocene (15.97–5.33 Ma). *Earth Sci. Rev.*  
695 112, 1–22.

696 Raddatz, T., Reick, C., Knorr, W., Kattge, J., Roeckner, E., Schnur, R., Schnitzler, K., Wetzzel, P.,  
697 Jungclaus, J., 2007. Will the tropical land biosphere dominate the climate-carbon cycle feedback  
698 during the twenty-first century? *Climate Dyn.* 29, 565–574.

699 Raddatz, J., Rüggeberg, A., Margreth, S., Dullo, W.-C., the IODP Expedition 307 Scientific Party,  
700 2011. Paleoenvironmental reconstruction of Challenger Mound initiation in the Porcupine  
701 Seabight, NE Atlantic. *Marine Geology* 282, 79–90.

702 Raymo, M.E., Grant, B., Horowitz, M., Rau, G.H., 1996. Mid-Pliocene warmth: stronger greenhouse  
703 and stronger conveyor. *Marine Micropaleontology* 27, 313–326.

704 Rhein, M., Rintoul, S.R., Aoki, S., Campos, E., Chambers, D., Feely, R.A., Gulev, S., Johnson, G.C., Josey,  
705 S.A., Kostianoy, A., Mauritzen, C., Roemmich, D., Talley, L.D., Wang, F., 2013. Observations: Ocean. In  
706 Stocker, T.F., Qin, D., Plattner, G.-K., Tignor, M., Allen, S.K., Boschung, J., Nauels, A., Xia, Y., Bex, V.,  
707 Midgley, P.M. (eds.). *Climate Change 2013: The Physical Science Basis. Contribution of Working*  
708 *Group I to the Fifth Assessment Report of the Intergovernmental Panel on Climate Change.*  
709 Cambridge University Press, Cambridge, United Kingdom and New York, NY, USA.

710 Rhines, P.B., Häkkinen, S., 2003. Is the oceanic heat transport in the North Atlantic irrelevant to the  
711 climate in Europe? *ASOF Newsletter* 1 (September 2003), 13–17.



712 Robinson, M.M., Dowsett, H.J., Dwyer, G.S., Lawrence, K.T., 2008. Re-evaluation of mid-Pliocene  
713 North Atlantic sea-surface temperatures. *Paleoceanography* 23, PA3213.  
714 doi:10.1029/2008PA001608.

715 Roeckner, E., Bäuml, G., Bonaventura, L., Brokopf, R., Esch, M., Giorgetta, M., Hagemann, S.,  
716 Kirchner, I., Kornblüeh, L., Manzini, E., Rhodin, A., Schlese, U., Schulzweida, U., Tompkins, A., 2003.  
717 The atmospheric general circulation model ECHAM5. part I : Model description. Tech. Rep. 349, Max-  
718 Planck-Institut für Meteorologie, Hamburg.

719 Salzmann, U., Haywood, A.M., Lunt, D.J., Valdes, P.J., Hill, D.J., 2008. A new global biome  
720 reconstruction and data-model comparison for the Middle Pliocene. *Global Ecology and*  
721 *Biogeography* 17, 432–447.

722 Salzmann, U., Dolan, A.M., Haywood, A.M., Chan W.-L., Hill, D.J., Abe-Ouchi, A., Otto-Bliesner, B.,  
723 Bragg, F., Chandler, M. A., Contoux, C., Dowsett, H.J., Jost, A., Kamae, Y., Lohmann, Lunt, D. J.,  
724 Pickering, S.J., Pound M.J., Ramstein, G., Rosenbloom, N.A., Sohl, L., Stepanek, C., Ueda, H, Zhang, Z.,  
725 2013. Challenges in reconstructing terrestrial warming of the Pliocene revealed by data-model  
726 discord. *Nature Climate Change* 3, 969–974,

727 Seager, R., Battisti, D.S., Yin, J., Gordon, N., Naik, N., Clement, A.C., Cane, M.A., 2002. Is the Gulf  
728 Stream responsible for Europe’s mild winters? *Q.J.R. Meteorol. Soc.* 128, 2563–2586.

729 Sepulchre, P., Arsouze, T., Donnadieu, Y., Dutay, J.-C., Jaramillo, C., Le Bras, J., Martin, E., Montes, C.,  
730 Waite, A.J., 2014. Consequences of shoaling of the Central American Seaway determined from  
731 modeling Nd isotopes. *Paleoceanography* 29, 176–189.

732 Shevenell, A.E., Kennett, J.P., Lea, D.W., 2004. Middle Miocene Southern Ocean cooling and Antarctic  
733 cryosphere expansion. *Science* 305, 1766–1770.

734 Spicer, R.A., Herman, A.B., Yang, J., Spicer, T.E.V., 2013. Why Future Climate Change is likely to be  
735 Underestimated: Evidence from Palaeobotany. *J. Botan. Soc. Bengal* 67(2), 75–88.

736 Stainforth, D.A., Aina, T., Christensen, C., Collins, M., Faull, N., Frame, D.J., Kettleborough, J.A.,  
737 Knight, S., Martin, A., Murphy, J.M., Piani, C., Sexton, D., Smith, L.A., Spicer, R.A., Thorpe, A.J., Allen,  
738 M.R., 2005. Uncertainty in predictions of the climate response to rising levels of greenhouse gases.  
739 *Nature* 433, 403–406.

740 Stepanek, C., Lohmann, G., 2012. Modelling mid-Pliocene climate with COSMOS. *Geosci. Model. Dev.*,  
741 5, 1221–1243.

742 Steph, S., Sturm, A., Tiedemann, R., 2006. Pliocene Reorganisation in Ocean Circulation. American  
743 Geophysical Union, Fall Meeting 2006, abstract.

744 Steppuhn, A., Micheels, A., Bruch, A.A., Uhl, D., Utescher, T., Mosbrugger, V., 2007. The sensitivity of  
745 ECHAM4/ML to a double CO<sub>2</sub> scenario for the Late Miocene and the comparison to terrestrial proxy  
746 data. *Global and Planetary Change* 57, 189–212.

747 Utescher, T., Bondarenko, O.V., Mosbrugger, V., 2015. The Cenozoic Cooling – continental signals  
748 from the Atlantic and Pacific side of Eurasia. *Earth and Planetary Science Letters* 415, 121–133.

749 Utescher, T., Bruch, A.A., Erdei, B., François, L., Ivanov, D., Jacques, F.M.B., Kern, A.K., Liu, Y.-S.,  
750 Mosbrugger, V., Spicer, R.A., 2014. The Coexistence Approach—Theoretical background and practical  
751 considerations of using plant fossils for climate quantification, *Palaeogeography, Palaeoclimatology,*  
752 *Palaeoecology* 410, 58–73.

753 Utescher, T., Böhme, M., Hickler, T., Liu, Y.-S.(C.), Mosbrugger, V., Portmann, F., 2013. Continental  
754 climate and vegetation patterns in North America and Western Eurasia before and after the closure  
755 of the Central American Seaway. In: GSA 125th Anniversary Annual Meeting. Denver. In: Geological  
756 Society of America Abstracts with Programs, vol.45, 7, p.302.

757 Utescher, T., Ashraf, A.R., Dreist, A., Dybkjær, K., Mosbrugger, V., Pross, J., Wilde, V., 2012. Variability  
758 of Neogene continental climates in Northwest Europe – a detailed study based on microfloras. *Turk.*  
759 *J. Earth Sci.*21, 289–314. <http://dx.doi.org/10.3906/yer-1005-3>.

- 760 Utescher, T., Bruch, A.A., Micheels, A., Mosbrugger, V., Popova, S., 2011. Cenozoic climate gradients  
761 in Eurasia – a palaeo-perspective on future climate change? *Palaeogeogr. Palaeoclimatol.*  
762 *Palaeoecol.*304, 351–358.
- 763 Utescher, T., Mosbrugger, V., Ivanov, D., Dilcher, D.L., 2009. Present-day climatic equivalents of  
764 European Cenozoic climates. *Earth and Planetary Science Letters* 284, 544–552.

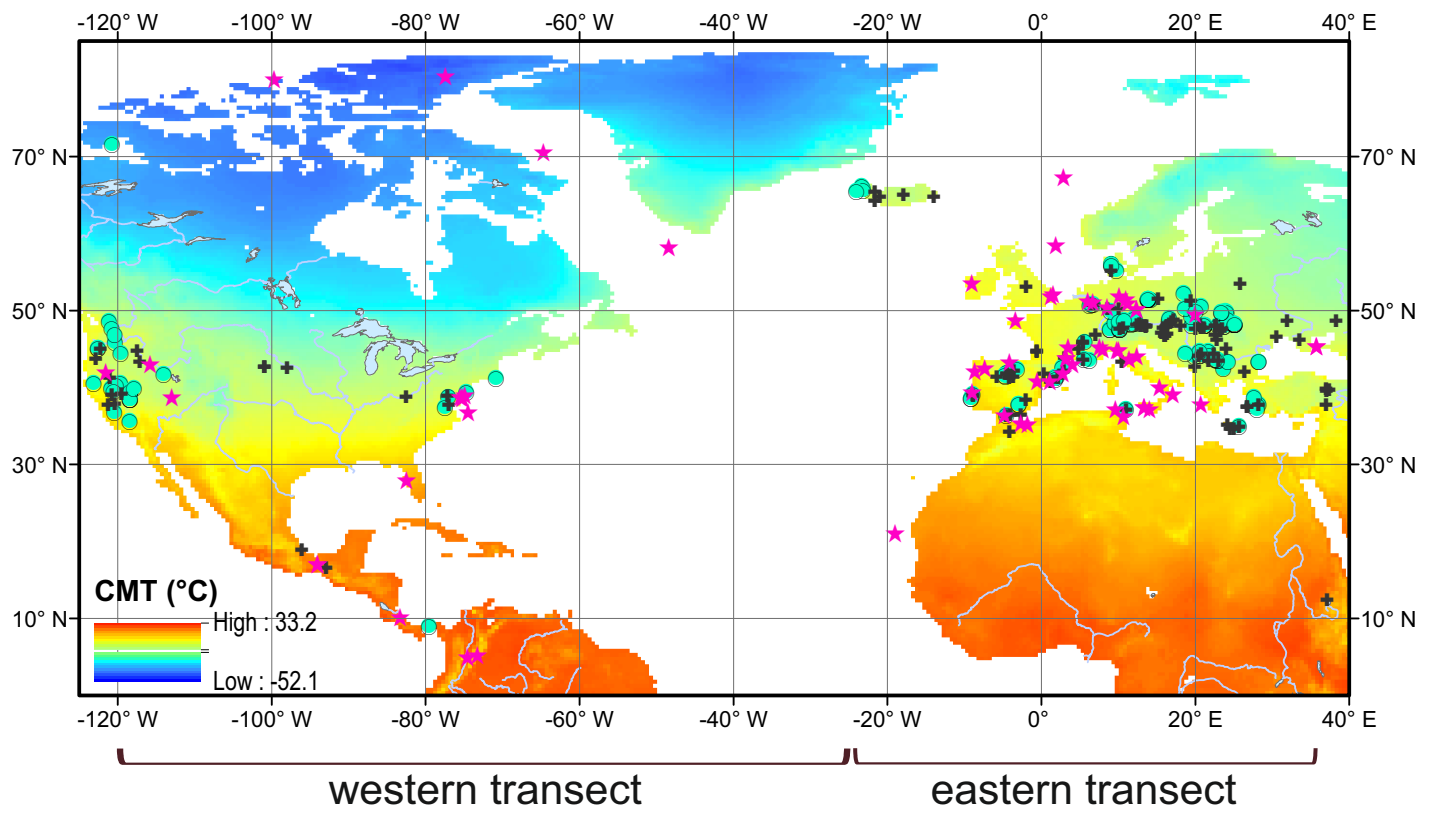


Figure 2  
[Click here to download Figure: Utescher\\_et\\_al\\_Continental\\_Climat\\_Patterns\\_Figure\\_2.pdf](#)

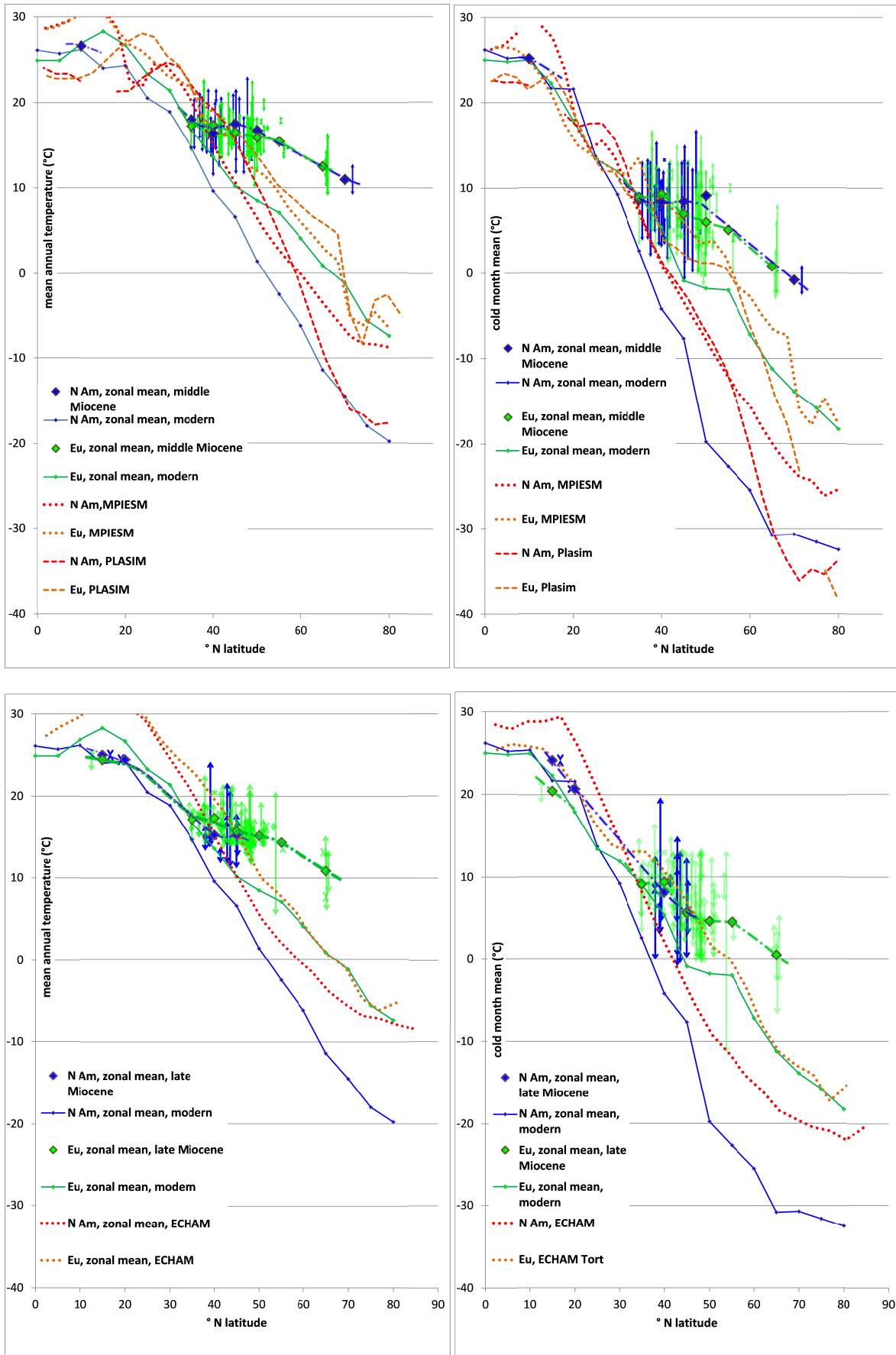


Figure 3

[Click here to download Figure: Utescher\\_et\\_al\\_Continental\\_Climate\\_Patterns\\_Figure\\_3.pdf](#)

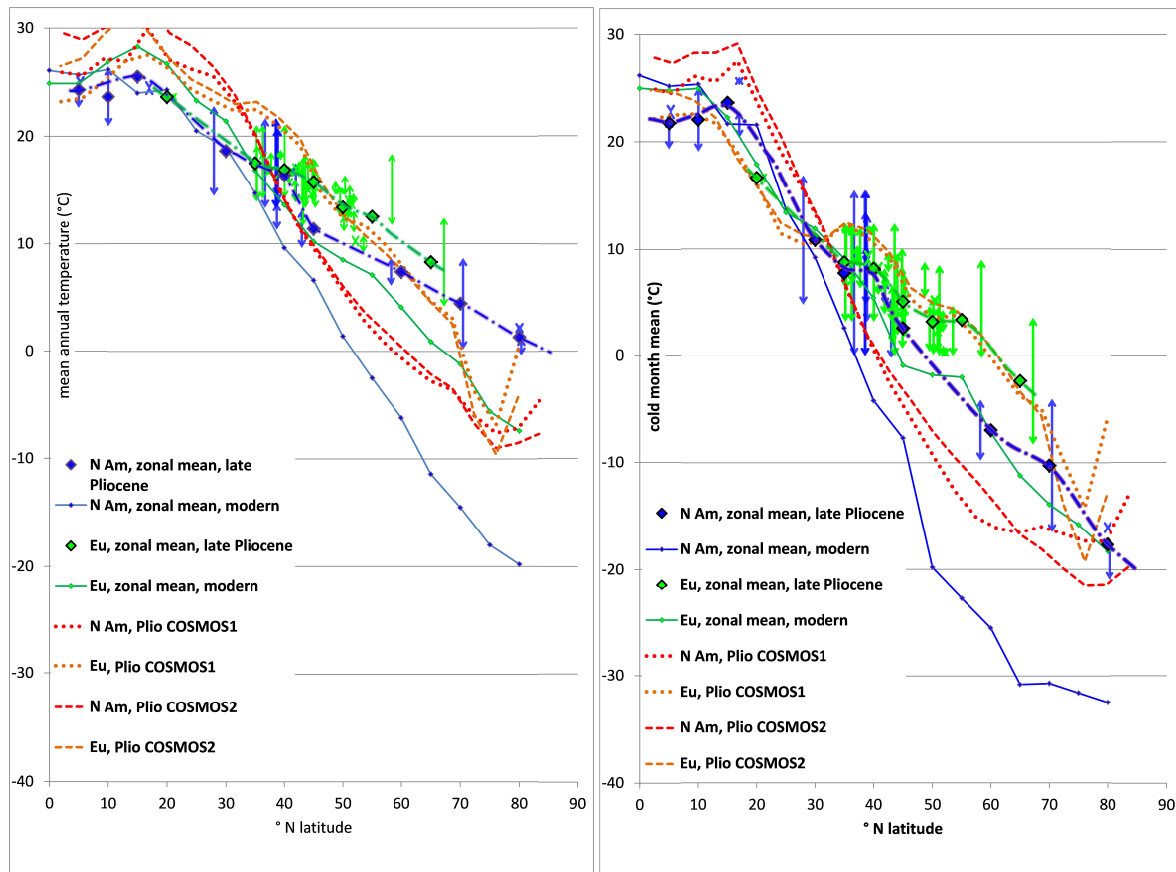


Table 1

[Click here to download Table: Utescher\\_et\\_al\\_Continental\\_Climate\\_Patterns\\_Table\\_1.docx](#)

Table 1: Selected GCM simulations and setup details

Models	Atmosphere	Ocean	Land surface	Palaeogeography	pCO <sub>2</sub>
<b>middle Miocene</b>					
<b>MPI-ESM</b> (Krapp and Jungclaus, 2011)	ECHAM5 (T42)	MPI-OM (fully coupled)	JSBACH (fully coupled)	from Herold et al. (2008)*	480 ppmv
<b>Planet Simulator</b> (Henrot et al., 2010)	PUMA-2 (T42)	SSTs and SICs prescribed from Butzin et al. (2011)	fixed vegetation from CARAIB run (Henrot et al., 2010)	from Butzin et al. (2011)*	500 ppmv
<b>late Miocene</b>					
<b>COSMOS</b> (Micheels et al., 2011)	ECHAM5 (T31)	MPI-OM (fully coupled)	fixed vegetation from proxy-based reconstruction (Micheels et al., 2007)	present-day based with adaptation to late Miocene (Micheels et al., 2011)**	360 ppmv
<b>late Pliocene</b>					
<b>COSMOS 1</b> (Stephanek and Lohmann, 2012)	ECHAM5 (T31)	SSTs and SICs prescribed from Dowsett et al. (2009)	fixed vegetation derived from the PLIOMIP protocol (Haywood et al., 2011)	derived from the PLIOMIP protocol (Haywood et al., 2011) ***	400 ppmv
<b>COSMOS 2</b> (Stephanek and Lohmann, 2012)	ECHAM5 (T31)	MPI-OM (fully coupled)	fixed vegetation derived from the PLIOMIP protocol (Haywood et al., 2011)	derived from the PLIOMIP protocol (Haywood et al., 2011) ***	400 ppmv

\* Middle Miocene configurations both include open Central American and Tethys Seaways, a closed Bering Strait and a filled Hudson Bay.

\*\* Late Miocene configuration includes an open Central American Seaway, the Paratethys and Pannonian Lake and a closed Hudson Bay.

\*\*\* Late Pliocene configuration includes closed Central American and Tethys Seaways, an open Bering Strait and a closed Hudson Bay.

**Supplementary material for online publication only**

[Click here to download Supplementary material for online publication only: Utescher\\_et\\_al\\_Continental\\_Climate\\_Patterns\\_supp](#)